

USE OF FIBER-OPTIC SENSOR TO RECORD PULSED PLASMA DISCHARGE CURRENT

A. G. Bedrin, A. N. Zhilin, and I. L. Lovchy

UDC 535.5, 53.082.5

The need to increase the precision with which the form of the pulse of the rapidly varying current of powerful plasma radiation is recorded under the conditions of powerful electromagnetic induction is considered. It is suggested that that a polarimetric fiber-optic current sensor based on a Spun-type light guide should be used to record powerful pulsed discharges. With the use of this type of current sensor it becomes possible to implement a technique of recording powerful pulse discharges of a plasma radiator in a regime of time profiling of the current pulse of two high-voltage capacitive storage devices with total energy up to 1800 kJ. The discharge chamber, power circuit, and evolution of the plasma discharge are described. The design and operating principle of a prototype of a two-pass polarimetric fiber-optic sensor with Spun-type optical cable and Faraday compensator that exhibits mutual optical anisotropy are presented. The general scheme of current measurements and the calibration circuit of the sensor are presented and experience gained from the use of a prototype of a sensor for measurement of powerful current pulses is described. Features of pre-calibration of the sensor are discussed. Results of a measurement of current by optical and traditional methods of recording based on the use of a Rogowski coil and Hall sensors are compared and a significant increase in the precision of reproduction of the shape of the current pulse by the optical method of recording is noted. Different modes of modernization of a fiber-optic sensor for expanding the range of recording current are considered.

Keywords: magnetoplasma discharge, Rogowski coil, Hall sensor, polarimetric fiber-optic current sensor, Spun optical fiber.

Introduction. Special galvanic decoupling anti-noise sensors (current sensors) are required to record the shape of the pulse of the rapidly varying current of a powerful plasma radiator under the conditions of powerful electromagnetic induction. However, the precision with which the shape of current pulses are recorded with the use of traditional current sensors is low, with the total error reaching possibly reaching 10%. The precision with which the shape of the current pulse of a powerful plasma radiator is recorded may be significantly increased (up to around 1–2%) with the use of fiber-optic current sensors (FOCS). FOCS possess a number of advantages: absence of saturation and hysteresis phenomena; ultra-low inertia; ideal galvanic isolation; ability to measure currents in conductors of complex design; versatility in measurements of variable and constant currents; and low mass and dimensional parameters. Therefore, these types of sensors should be used in systems that record high-voltage pulsed current processes, in particular, in the measurement of powerful pulse currents that occur in the discharge of a magnetoplasma compressor [1], such as a plasma radiator incorporated into a test bench used to simulate the radiation of a high-altitude, high-temperature manmade source [2]. Simulation of a specific spectral-energy and time distribution of the radiation of a plasma source is achieved by means of controlled diversity in the course of discharges of high-voltage capacitor stores in a common discharge chamber with controlled composition and pressure of a gas medium. Besides traditional gas sensors, such as the Rogowski coil and Hall sensor, a test bench detection system includes a two-pass polarimetric fiber-optic current sensor [3] based on a Spun-type optical cable (henceforth, Spun optical cable) with Faraday compensator exhibiting mutual optical anisotropy. A stable growth in the industrial and scientific use of fiber-optic current sensors is observed abroad [4–6].

TABLE 1. Parameters of Two Types of Capacitive Energy Stores

Parameter	ENE-78	Sections of INE-2M		
Capacitance, mF	0.25	48	48	12
Charging voltage, kV	25	5	5	10
Maximal storable energy, kJ	78	1800		
Period/length, μ sec	58	500–5000		
Maximum current, kA	5800	1300		

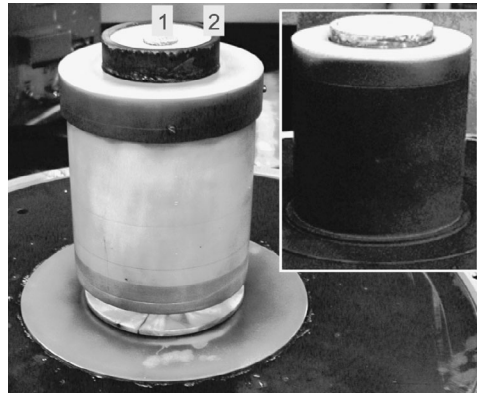


Fig. 1. Bases of discharge chamber with electrodes before and following (inset) a series of electrical discharges: 1) central electrode; 2) cylindrical conductive body.

The objective of the present article is to describe experience gained with the use of a polarimetric fiber-optic sensor in a system designed to record powerful pulse currents and compare the results of a measurement of current by optical and traditional electromagnetic sensors.

Test bench for simulating high-temperature processes. The bases of a discharge chamber with electrodes before and after a series of electric discharges (inset) are shown in Fig. 1. The discharge of a magnetoplasma compressor is generated in the upper part of a pedestal between the central electrode 1 and a cylindrical conductive body 2. High-voltage coaxial cables with internal cores are distributed around the perimeter of the basis of the chamber and shielding conductors connected to the central electrode are used as a powerful (discharging) force conductor. Strong electrical erosion of the surface of the electrodes and an increase in the volume of the dust content of the walls and windows of the chamber with erosion products is observed following a high-energy discharge (cf. Fig. 1). In fact, the windows of the chamber must be cleaned following each trial in order to adequately record the spectrum of the plasma radiator. This leads to the need for lengthy preparatory stages when conducting experiments with a plasma radiator, which encourages the use of a test bench diagnostic equipment complex capable of achieving precise and noise-proof recording of the electrical and optical parameters in a single trial. The parameters of an electrolytic radiator with ENE-78 and INE-2M stores [2] are presented in Table 1. The ENE-78 store, which is characterized by a contribution to the discharge of high peak power, is used for preliminary tuning of the recording system. The INE-2M store consists of three sections and may be used generate discharge currents with amplitude up to 1.3 MA and length up to 5 msec. Management of the time parameters of the discharge current is achieved by controlled delay of the discharge times of the sections of the store, installation in the sections of additional generating elements in the sections, and variation of the load parameters in the discharge chamber.

In order to adequately record the time form of the current pulse by means of a traditional Rogowski coil meter, an integrating circuit with time constant more than 20 times the length of the recorded current [7] must be placed at the exit of a traditional meter. Therefore, to transmit the power from an ENE-78 store to an INE-2M store the parameters of the integrating circuit are increased 30-fold, which accompanied a proportional drop in the absolute sensitivity of the test bench-type

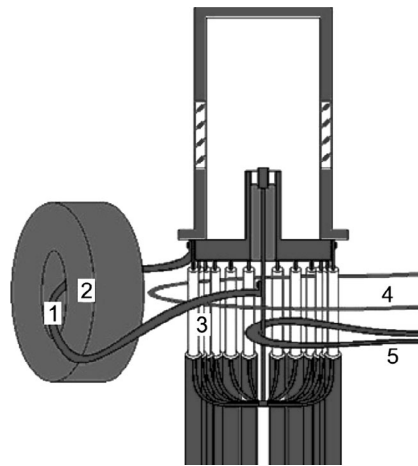


Fig. 2. Schematic diagram of discharge chamber, location of measurement circuits, and of live conductors: 1) short-circuit loop; 2, 5) case model test and bench Rogowski coil, respectively; 3) return conductors; 4) fiber circuit of fiber optic current sensor.

traditional meter employed and an increase in the noise component from the electromagnetic commutator noise in the form of the recorded current pulse. A schematic diagram of the cross-section of discharge chamber and the relative position of the measurement loops and live conductors – the fiber circuit of the fiber optic current sensors 4, reverse current conductors 3, and shorting loops 1 – is presented in Fig. 2. Structurally, flexible implementation of a test bench Rogowski coil 5 due to the need for its placement in the small space between the high-voltage live conductors, is caused by insufficiently careful shielding of its measurement circuit against external electromagnetic noise. The shielding of the test bench Rogowski coil is substantially worse than the shielding of the body model Rogowski coil (model Rogowski coil) 2, though because of the overall dimensions of the latter it cannot be directly used in experiments with a plasma source. A model Rogowski coil is used only in calibration of a test bench Rogowski coil in a shorting energy store regime.

Fiber optic current sensors based on a Spun optical fiber. The physical mechanism underlying the measurement of the current of a fiber-optic current sensor is based on the Faraday magneto-optical effect, i.e., rotation of light polarization plane in a magnetic field of the conductor with current described by the formula

$$\alpha_F = V \int_L H_l dl = VNi,$$

where α_F is the angle of rotation of the polarization plane of light that has passed through a closed fiber-optic loop of length L around a waveguide L units in length around a conductor with current i ; H_l – component of magnetic field of conductor with current in the direction of polarization of light; V – Verdet's constant of the optical material of the waveguide; and N – number of loops of waveguide circuit around a conductor transmitting a current.

The development of glass-fiber sensors, the first models of which appeared more than 40 years ago, began with annealing of a sensitivity circuit made of quartz fiber or with the use in the circuit of fiber of flint glass with low elasto-optical coefficient, with the use of special forms of coils of fiber in the winding with alternate rotation of a plane of windings by 90° . Such measures were adopted in order to level out the influence of knees of fiber in the coil by the sensitivity of the sensor. Twist- or Spun-optical cables, which exhibit very strong internal birefringence, are chiefly used in modern sensors. The former type is characterized by circular birefringence induced by elastic torsion of isotropic fiberglass about its axis and the second type, by linear torsion with helical structure induced by a process of thermal stretching of fiber produced by a turned billet with strong birefringence. The strong ordered birefringence levels out the influence of the external elasto-optical effects on the Faraday effect, though it limits the sensitivity of the magneto-optical sensor, unlike the sensitivity of a sensor with virtual ideal isotropic fiberglass in which there exists only circular Faraday birefringence. In practical applications, therefore, a light guide with required parameters is selected as the physical dimension of the sensing circuit of the sensor in order to assure acceptable levels of sensitivity and stability of the sensor or the dimensions of the circuit of the existing optical cable

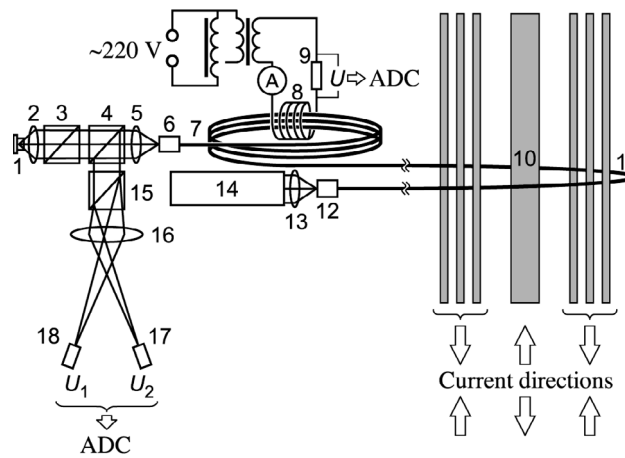


Fig. 3. Structure of fiber-optic current sensor and pre-calibrator circuit: 1) radiation; 2, 5, 13) microscope objectives; 3, 4) polarization and polarization-neutral (50/50) beam-splitting cubes, respectively; 6, 12) optical connectors; 7) optical fiber; 8) solenoid; 9) high-precision low-resistance shunt; 10, 11) main and return current conductors of discharge chamber; 14) conditional case; 15) Wollaston polarizing cube; 16) lens; 17, 18) photodiodes; ADC – alpha-to-digital converter.

are adjusted. Commercial interferometric fiber sensors for measurement of currents in the range 1–300 kA with error below 0.1% are described in [8]. In [9] a domestically produced design of a fiber-optic sensor for measurement of currents in the range 15–250 kA with error not greater than 0.5% is described. However, such sensors have yet to achieve widespread use in domestic industry or in applications in physical experiment. The use of a prototype of a two-pass polarimetric fiber optic current sensor [3] with Spun optical cables and Faraday compensator with mutual optical anisotropy for measurement of powerful pulse currents is described in the present article.

Let us now present some information about Spun optical cables. A typical birefringent beat length L_β and step length L_τ of twisting of a fiber amount to several millimeters, with $L_\tau \leq L_\beta$. A decrease in the beat length L_β increases the stability of the response of the sensor to curvatures of the fiber in space, while an increase in the ratio L_β/L_τ increases the sensitivity of the sensor. A Spun-optical cable of a prototype of a fiber optic current sensor exhibits the following parameters: $L_\beta = 4$ mm (at the wavelength of the radiation of an optical beam $\lambda = 660$ nm) and $L_\tau = 3.3$ mm. With these parameters the theoretical relative sensitivity of the sensor η in the case of low currents amounts to roughly 87% of the maximally possible (relative to the sensitivity of a sensor with ideal isotropic fiber) with possible deviations of the sensitivity not greater than $\pm 0.5\%$ in the case of a radius of bending of the optical cable not greater than 35 mm [3].

The prototype of the sensor consists of an opto-electronic block of radiation input of a supermode laser diode in an optical cable and recording of the intensity of orthogonally polarized components of optical radiation returned from the circuit, an opto-mechanical block of return radiation input to the optical cable accompanied by rotation of the state of polarization by 90° and a laptop computer with independent board of a USB-6351-NI 16-digit analog-to-digital converter (National Instruments, USA) with maximal response frequency of the channels 1.25 MHz. The optical blocks are connected by a Spun optical fiber with standard FC/APC connectors at their ends. A computer is used to monitor the radiant intensity (relative to the voltage of a built-in photodiode) and current (relative to the voltage of the load resistance in the power-supply circuit) of a laser diode, and digitization and processing of the measurement signals from the photodiodes. A sensor interface was developed in a LabVIEW graphical programming environment. The power of the computer, radiator, and detector is produced by an autonomous store. The overall length of the Spun optical fiber reaches 20 m, which makes it possible to situate a metallic cabinet with optical sensor and computer outside the site (bin) of the discharge chamber.

The structure of a fiber optic current sensor and its pre-calibration circuit is represented in Fig. 3. The sensor functions in the following way. Radiation from the laser diode 1 is collimated by the microscope objective 2, filtered by the polarization beam-splitting cube 3, travels through the polarization-neutral beam-splitting cube 4 (50/50) and focused by the microscope objective 5 through an optical connector 6 in the core of the optical fiber 7. In order to calibrate the sensitivity

of the sensor, the optical cable is passed three times through a solenoid 8 consisting of 4476 loops of a wire conductor with electric power supplied by an auto-converter that passes through a step-down transformer. The maximal effective value of the current in the solenoid reaches 6.3 A, which makes it possible to simulate in the course of calibration an amplitude strength of the current passing through the optical cable circuit of up to 120 kA. A high-precision low-resistance shunt 9 in its power circuit with voltage measured by an alpha-numeric converter is used to measure the current of the solenoid.

The optical cable forms a sensing circuit around the main conductor 10 and (or) some of the return conductors 11 of the discharge chamber. The number of return conductors included, which depends on the proposed maximum measured current, is adjusted in the course of the experiments.

After passing through the sensing circuit, the probe radiation with polarization state transformed as a result of the combined action of the integral spiral linear birefringence of optical cable 12 and the magneto-optical Faraday effect, enters the independent reverse radiation input block through connector 12 in a fiber where it is collimated by the microscope objective 13. The radiation then travels twice through an anisotropic birefringent crystal and magneto-optical glass situated inside a permanent cylindrical magnet with intermediate reflection by a mirror (in Fig. 3 these elements are situated in the conditional case 14) and is again focused by microscope objective 13 in the optical cable with the polarization state changed to the orthogonal. This type of operation is needed to stabilize the working point of the sensor in the course of measurements, since in this state the rapid and slow axes of linear birefringence are interchanged in the optical cable in order to achieve reverse radiation. In the absence of current in the circuit the state of polarization of radiation that has traveled in the reverse direction through the optical cable returns to the linear, orthogonal state of polarization of the input light, independently of possible changes in the spectral, temperature, and geometric conditions of the measurements.

In the course of traveling in the reverse direction through the optical cable circuit, the action of the Faraday effect in the circuit of the optical cable is duplicated. The probe radiation travelling through the capacitor 6 exits the optical cable and is collimated in the microscopic objective 5, and partially reflected by the diagonal face of the polarization-neutral beam splitter 4, enters the analyzer. The analyzer – a Wollaston polarizing cube 15 – is mounted at an angle of $\pm 45^\circ$ to the plane of polarization of the light which the radiation in the light is divided into two light beams with orthogonal linear polarization. The beams are focused the lens 16 into the sensitive areas of the photodiodes 17 and 18 which function in a photodiode regime. The voltage of the load resistances in the power circuits of the photodiodes (measurement signals) are digitized by means of an alphanumeric converter. Some of the radiation that has passed through the neutral beam splitter 4 is separated by the diagonal face of the polarized beam splitter 3 laterally. Thus, optical bypassing of the resonator of the diode laser from the external mirror of the return input block of the radiation is achieved. Similar descriptions of a prototype of the fiber-optic current sensor and its operation are presented in [3].

Algorithm for processing measurement signals and range of measurement of currents of fiber-optic current sensors. In a virtual ideal isotropic fiber, current i is determined by the sensor by means of the expression

$$i = \arcsin(\Delta U_{12})/(4NV), \quad (1)$$

where $\Delta U_{12} = (U_1 - U_2)/(U_1 + U_2)$ is the relative difference between the measurement signals U_1 and U_2 of the photodiodes.

With the use of the relative difference between the measurement signals in the processing algorithm, it becomes possible to eliminate the influence of variations in the radiant intensity in the course of the measurements. This is especially critical in the measurement of strong currents. In this case, reverse radiation in the emitter (in the present device, a laser diode) partially penetrates through a polarization splitter from the optical cable circuit, forming a weak optical connection of the resonant cavity of the laser diode with an external mirror. This leads to some modulation relative to the radiant strength of the laser diode, that is, the radiant strength of the signals U_1 and U_2 . However, the relative difference between the measurement signals remains unchanged.

In the case of a single-coil circuit produced from an ideal isotropic fiber, the range of a single-valued measurement of the currents is bounded by Eq. (1) by the two limits,

$$-(\pi/2)/(4V) < i < (\pi/2)/(4V).$$

With $V \approx 4.3 \mu\text{rad/A}$ for a quartz fiber in the case of wavelength $\lambda = 660 \text{ nm}$, the range is limited roughly to $\pm 91 \text{ kA}$. In a physical Spun optical fiber, the dependence $i(\Delta U_{12})$ corresponds to (1) (with scale factor η) only within the range of a

relatively short segment. The functional dependence then becomes complicated, moreover, the range of the well-defined correspondence of the magnitude of the difference ΔU_{12} to the current strength i may vary. In particular, for the Spun optical fiber sensor used in the prototype this range corresponds to roughly -93 to $+98$ kA (the asymmetry of the range is apparently due to the fact that the direction of polarization of the input radiation does not correspond to the direction of one of the axes of internal birefringence on the inlet side of the optical cable or is at an angle of $\pm 45^\circ$ to this direction). From the edges of the range the precision of the measurements decreases as a consequence of the fact that the ratio of the increment in the difference ΔU_{12} to the increment in the current i tends to zero. Therefore, the calibration curve of the sensor – the dependence of the relative difference of the measurement signals ΔU_{12} from the instantaneous value of the current i – was constructed in the range ± 80 kA. Moreover, the uncertainty of the response of the sensor, due principally to the noise of the strength of the laser diode, ranged principally from ± 100 A at low currents and up to ± 300 A at the edges of the range of calibration with the use of the measurement signals of the autonomous board of the alpha-numeric converter. As regards the experiments designed to increase the rate of extraction of information, the measurement signals of the photodiodes were digitized by means of a TDS1002 digital storage oscillograph (Tektronix, United States) with maximal digital sampling frequency 1 GHz and digitization word length 8 bits. In this case, the uncertainty of the measurement results increases roughly ten-fold.

The actual range of the discharge currents of a magnetoplasma compressor is significantly broader than a range of ± 80 kA, hence the fiber circuit encompasses the main conductor and (or) some of the return live conductors.

Results of experiments. The actual calibration curve of the sensor $\Delta U_{12}(i)$ was constructed immediately prior to performing the next cycle of experiments in the range of currents ± 80 A. Based on a ninth-degree polynomial this curve was transformed into an inverse functional relationship $i(\Delta U_{12})$ and used subsequently to process the measurement signals of the sensor in order to determine the current strength.

The results of recording the radiator current by means of a Rogowski coil (RC) and fiber-optic current sensor (FOCS) with voltage of the ENE-78 store of 15.1 kV and coverage by sensing circuits of only the main conductor are presented in Fig. 4. The sampling rate of the signals is 25 MHz while the maximum amplitude of the current reaches 325 kA. By Eq. (1), in this case, the response of the fiber-optic current sensor is ambiguous. In the case of imaginary reflection of “descending” fragments relative to levels $+98$ ($+289$) and -93 kA, the forms of the response curves of the Rogowski coil and the fiber-optic current sensor practically coincide (the “reflected” fragments are displayed in green) in addition to the initial segment, where the scatter of the current strengths measured by the Rogowski coils are substantially greater. Therefore, in each subsequent trial the sensing circuit of the fiber-optic current sensor encompasses the main conductor and (or) some of the return conductors to enable penetration of the total current that travels through the optical cable circuit in the range ± 80 kA. In this case, the fiber-optic current sensor is used only for precise recording of the time form of the current, since the adequacy of the absolute values is due to the true weight distribution of the currents across the return conductors.

The absolute sensitivity of the test bench Rogowski coil is determined by means of the model Rogowski coil (MRC) 5 from trials with short-circuiting of the ENE-78 store circuit (with charging voltage $U_{ch} < 7$ kV; at higher voltages of the store the shorting regime breaks down as a consequence of partial development of parallel plasms discharge). Because of the greater overall dimensions of the model Rogowski coil, it cannot be used in experiments with plasma discharge. In the power regimes of the ENE-78 store, the sensitivity of the Rogowski coil and of the model Rogowski coil amount to 54 and 16.3 kA/V, respectively.

The results of a measurement of the current in a shorting regime by a Rogowski coil, model Rogowski coil, and fiber-optic current sensor with storage voltage 7 kV are presented in Fig. 5 with signal sampling rate of 10 MHz. An increase in the rate of oscillation of the current by comparison with the preceding experiment is caused by the variation of the inductance of the discharge circuit due to insertion of an additional conductor in order to encompass the model Rogowski coil. The response of the fiber-optic current sensor was scaled to the levels of the readings of the Rogowski coil and model Rogowski coil. The initial fragment of the results of measurements is presented in a magnified scale in the inset of Fig. 5. From the signal/noise ratio, the response of the fiber-optic current sensor roughly corresponds to the model Rogowski coil, though it substantially exceeds that of the test bench Rogowski coil.

Hall sensors were used to measure the discharge current only in the radiator power supply regime from an INE-2M store. The sensors were situated in each of the three sections of the capacitative store and recorded the current in one of the

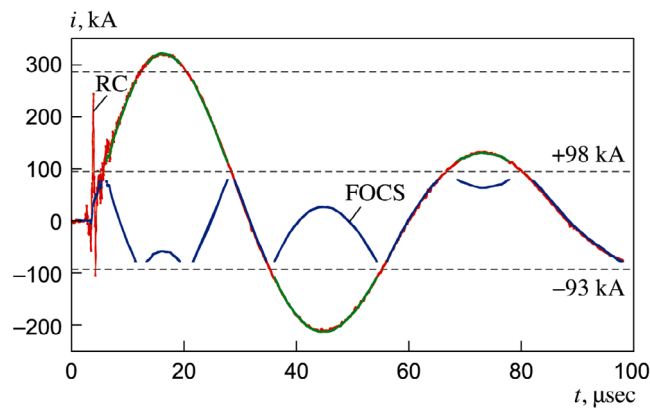


Fig. 4. Results of recording of the emitter current by means of fiber-optic current sensor with voltage of the ENE-78 store of 15.1 kV and coverage of the sensing circuits of the main conductor; “reflected” fragments highlighted in green.

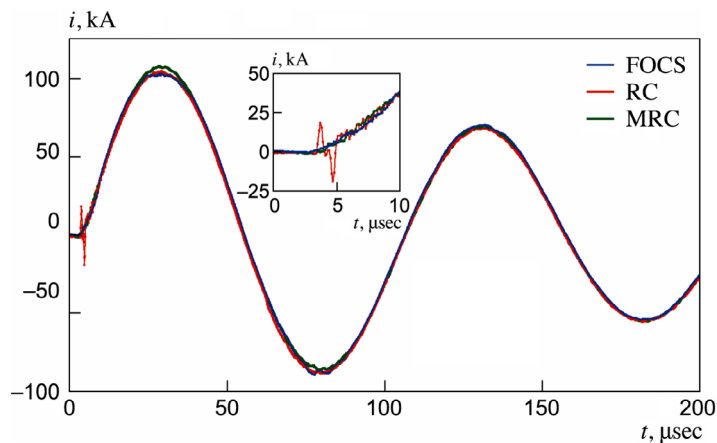


Fig. 5. Results of recording the current in a shorting regime by means of a Rogowski coil, model Rogowski coil, and fiber-optic current sensor at a storage voltage of 7 kV.

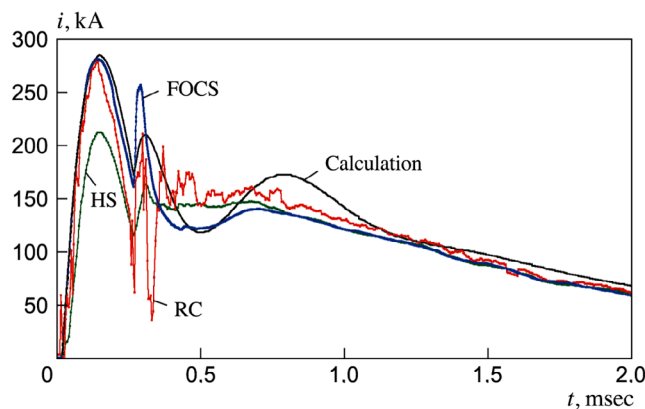


Fig. 6. Calculated curve and curves measured by means of ROCS, RC and Hall sensors (HS) of the emitter current waveform for the case of power supply from three sections of the INE-2M store.

68 cables of the commutator. An amplitude of the output signal of 4 V with primary current in the range 1.5–2.5 kA and saturation of the output signal at a level of 10 V are typical conversion parameters for these sensors. The frequency working range of the sensors reaches 25 kHz. The total current in the plasma load is calculated by summing the data from three Hall sensors and multiplying the result by 68. The potentially possible nonuniformity of the distribution of the currents across the cables of the commutator served as the source of an additional error of the record of the total error.

The calculated curve and curves that were measured by a fiber-optic current sensor, test bench Rogowski coil with sensitivity 1600 kA/V, and Hall sensors of the emitter current waveform for the case of power supply from three sections of an INE-2M store are presented in Fig. 6. The alphanumeric converter has a query rate of 1.25 MHz. The parameters of the store are as follows: capacitance of first section $C = 12$ mF; charging voltage $U_{\text{ch}} = 4.5$ kV; second and third sections of total capacitance $C = 96$ mF, $U_{\text{ch}} = 3.25$ eV. The start up delay of the second and third sections of the INE-2M store relative to the first reaches 250 μsec . A constant resistance of 5 m Ω was used in place of the nonlinear resistance of the plasma load when the discharge current was calculated in the MicroCap program. The form of the current reproduces maximally adequately a fiber-optic current sensor with high-grade “tracing” of the peak at the start of the second and third sections of the store. A corresponding peak is also observed in the radiation of a plasma discharge when recorded by a photoelectronic multiplier. This peak of the current is distorted when it is recorded by a measurement Rogowski coil or Hall sensor due to the extraordinarily large noise component of the signal and the low amplitude-frequency characteristics, respectively. The forms of the rear front of the current pulse of all the sensors roughly coincide 0.7 msec after the start of a discharge. The difference in the computed curve of the current from the form recorded by a fiber-optic current sensor is apparently related to the replacement in the calculations of the physical resistance, especially the nonlinear reactive resistance of the discharge plasma, by some fixed value of the resistance.

Conclusion. With the use of fiber-optic current sensors it becomes possible to significantly increase the precision with which the form of the current pulse of a powerful plasma radiator is recorded as compared to the use of traditional current sensors. An essential theoretical constraint of the range of measured currents at a level of around ± 90 kA is a drawback of the prototype of the fiber-optic current sensor employed, making it necessary to partially cover the return live conductors in the course of an experiment. One possible alternative design to the construction of an optical recording system for measurement of the absolute level of the current is to use several fiber-optic current sensors with batch coverage of the return conductors with the sum of the currents of these cables equal *a priori* to the total current. Another alternative design is to use a laser diode that functions in the infrared range of the spectrum. In view of the roughly quadratic inverse dependence of the Verdet constant on the wavelength of the radiation, in a transition to a wavelength of 1550 nm the range of measurement of the current may potentially be expanded more than five-fold.

REFERENCES

1. A. S. Katrukov, N. P. Kozlov, and Yu. S. Protasov, “Continuous spectrum plasmodynamic sources,” *DAN SSSR*, **239**, No. 4, 831–834 (1978).
2. A. G. Bedrin and A. N. Zhilin, “Test bench for simulation of optical radiation from a high-temperature source,” in: *Proc. 9th Int. Symp. on Radiation Plasmodynamics*, Zvenigorod, Dec. 2012, Moscow, NITs Inzhener (2012), pp. 150–155.
3. I. L. Lovchii, “Numerical simulation and the study of a polarimetric current sensor with Spun-type optical cable,” *Opt. Zh.*, **77**, No. 12, 25–33 (2010).
4. A. J. Schwab, *Hochspannungsmesstechnik Messgerate und Messverfahren* [Russian translation], Energoatomizdat, Moscow (1983).
5. M. Willsch, R. Menke, and T. Bosselmann, “Magneto-optic current transformers for applications in power industry,” in: *Proc. 2nd Congr. of Optical Sensor Technology (OPTO 1996)*, Leipzig, Germany, Sept. 25–27, 1996.
6. T. X. Nguyen, J. E. Ely, and G. N. Szatkowski, in: *Proc. SPIE 9480, Fiber Optic Sensors and Applications, XII*, 94800X, May 13, 2015, <https://doi.org/10.1117/12.2172195>.
7. A. Gusarov, W. Leysen, M. Wuilpart, and P. Megret, *Fus. Eng. Design*, **136**, Part A, 477–480 (2018), <http://doi.org/10.1016/fusengdes.2018.03.001>.
8. K. Bohnert, G. Philippe, B. Hubert, and P. Guggenbach, “Highly accurate fiber-optic DC current sensor for the electrowinning industry,” *IEEE T. Ind. Appl. Mag.*, **43**, 180–187 (2005).
9. N. I. Starostin, M. V. Ryabko, Y. K. Chamorovskii, et al., *Key Eng. Mater.*, **437**, 314–318 (2010), <https://doi.org/10.4028/www.scientific.net/KEM.437.314>.